Characterization of CeO_2−ZrO_2 Mixed Oxides. Comparison of the Citrate and Sol−Gel Preparation Methods

M. Alifanti, B. Baps, N. Blangenois, J. Naud, P. Grange, and B. Delmon*

Unité de Catalyse et Chimie des Matériaux Divisés and Unité de Géologie, Université catholique de Louvain, Louvain la Neuve, Belgium

Received July 29, 2002. Revised Manuscript Received October 8, 2002

CeO_2−ZrO_2 mixed oxides were synthesized by two mild chemical routes: complexation with citric acid and the sol−gel method. XRD and ESEM investigations revealed the appearance of a solid solution around 400 °C, depending on the ratio between the two oxides and the preparation method. Solids obtained by the citrate method were more homogeneous on the whole range of composition. Solid-state investigations of the prepared materials did not show segregation of cerium or zirconium oxides, except in the high Ce ranges for samples prepared by the sol−gel method. The thermal stability of both oxides was enhanced by mutual substitution. The most stable solid solutions were obtained in the range 50 < Ce < 90% mol.

Introduction

Cerium containing materials, and especially cerium oxide, are used for different catalytic processes. The major role of ceria in three-way catalysts (TWC) is well-known. Because of its redox and acido-basic surface properties, it is also employed in fluid catalytic cracking, SO_x removal, ethylbenzene dehydrogenation, and the water gas shift reaction.[1,2] For this reason, the interest for this rare earth oxide has grown constantly, but this was mainly due to its use in automotive exhaust control. The main problem to be solved was the low stability in high temperature ranges. It is well-known in the ceramic industry that sintering and densification widely change as a function of the oxido-reduction state of the material. Actually, relations between structural modifications and the sintering process are strongly affected by the redox properties of ceria.[3] One way to stabilize the structure is to associate cerium oxide to other elements for obtaining solid solutions with improved thermal properties.[4,5] Recent studies reported the improvement of textural, redox, oxygen storage, and consequently, catalytic properties by introducing doping elements in the CeO_2 fluorite-type lattice. These doping elements were Al, Si, La, Y, Hf, Gd, and Zr.[4,6−10] It seems that the most efficient dopant is zirconium. Excellent studies of the Ce−Zr−O system were performed by Trovarelli et al.[11−14] and Fornasiero et al.[15−18] in the last 7 years. One of the difficulties in handling this system is the large variety of crystalline structures that may exist depending on the temperature and composition[19] and the corresponding impact that each type of crystallographic modification has upon the catalytic activity.

Actually, the range of temperatures in which textural characteristics and structural stability are useful for practical applications often corresponds to phase metastability with respect to the phase diagram.[19] The use of stabilized zirconia (in particular Ce-stabilized) in the field of ceramics has demonstrated that phases in the metastable range of composition can actually be stable for practical purposes. Obtaining one Ce−Zr−O phase or another depends on both the preparation method and the relative proportion of the elements. It is generally accepted that below 20% CeO_2 a monoclinic phase is formed, whereas for more than 70% ceria a solid solution

* Corresponding author. E-mail: delmon@cata.ucl.ac.be.

(1) Trovarelli, A. *Catal. Rev. Sci. Eng.* **1996**, *38*, 439.
(2) Trovarelli, A.; de Leitenburg, C.; Boaro, M.; Dolcetti, G. *Catal. Today* **1999**, *50*, 353.
(3) Schmieg, S. J.; Belton, D. N. *Appl. Catal. B: Environ.* **1995**, *6*, 127.
(4) Vidmar, P.; Fornasiero, P.; Kašpar, J.; Gubitosa, G.; Graziani, M. *J. Catal.* **1997**, *171*, 160.
(5) Sato, T.; Dosaka, K.; Yoshioka, T.; Okuwaki, A. *J. Am. Ceram. Soc.* **1992**, *75*, 552.
(6) Bensalem, A.; Bozon-Verduraz F.; Delamar, M.; Bugli, G. *Appl. Catal. A: General* **1995**, *121*, 81.
(7) Rocchini, E.; Trovarelli, A.; Llorca, J.; Graham, G. W.; Weber, W. H.; Maciejewski, M.; Baiker, A. *J. Catal.* **2000**, *194*, 461.
(8) Zamar, F.; Trovarelli, A.; de Leitenburg, C.; Dolcetti, G. *Stud. Surf. Sci. Catal.* **1996**, *101*, 1283.
(9) Pijolat, M.; Prin, M.; Soustelle, M.; Touret, O.; Nortier, P. *J. Chem. Soc., Faraday Trans.* **1995**, *91*, 3941.
(10) Duh, J.-G.; Dai, H.-T.; Chiou, B.-S. *J. Am. Ceram. Soc.* **1988**, *71*, 813.
(11) Maschio, S.; Trovarelli, A. *Br. Ceram. Transac.* **1995**, *94*, 191.
(12) Trovarelli, A.; de Leitenburg, C.; Dolcetti, G. *Chemtech* **1997**, 32.
(13) Trovarelli, A.; Zamar, F.; Llorca, J.; de Leitenburg, C.; Dolcetti, G.; Kiss, J. T. *J. Catal.* **1997**, *169*, 490.
(14) de Leitenburg, C.; Trovarelli, A.; Llorca, J.; Cavani, F.; Bini, G. *Appl. Catal. A: General* **1996**, *139*, 161.
(15) Fornasiero, P.; Di Monte, R.; Ranga Rao, G.; Kašpar, J.; Meriani, S.; Trovarelli, A.; Graziani, M. *J. Catal.* **1995**, *151*, 168.
(16) Fornasiero, P.; Balducci, G.; Di Monte, R.; Kašpar J.; Gubitosa, G.; Ferrero, A.; Graziani, M. *J. Catal.* **1996**, *164*, 173.
(17) Fornasiero, P.; Balducci, G.; Meriani, S.; Di Monte, R.; Graziani, M. *Catal. Today* **1996**, *29*, 47.
(18) Fornasiero, P.; Kašpar, J.; Sergo, V.; Graziani, M. *J. Catal.* **1999**, *182*, 56.
(19) Yashima, M.; Arashi, H.; Kakihana, M.; Yoshimura, M. *J. Am. Ceram. Soc.* **1994**, *77*, 1869.

10.1021/cm021274j CCC: $25.00 © 2003 American Chemical Society
Published on Web 12/24/2002

with a cubic symmetry appears. Between these limits, structures with cubic or tetragonal symmetries are obtained, with the formation of one or another being linked with the synthesis method and the thermal treatment to which the sample is submitted. A major challenge is to identify these phases because XRD patterns are very similar.[20] In relation to catalytic properties, oxygen mobility is favored by a cubic geometry, whereas the tetragonal or monoclinic symmetries limit its mobility through the lattice.[12,13,15]

The objective of the present study was to describe preparation methods for associating cerium and zirconium oxides and to characterize the corresponding materials. The major incentive for the present work is also to improve the cerium oxide textural properties, with special focus on its stabilization at high temperature. The influence of the molar Ce/Zr ratio upon the structural properties of the Ce−Zr−O system is investigated. The aim is therefore to get more information about the relative solubility of the two oxides in solids with a surface area, sufficiently high to be suitable for catalytic use. The aim of obtaining high surface areas implies that the calcination temperatures be considerably lower than usually reported, especially in studies concerning ceramics.

Experimental Section

Catalyst Preparation. The citrate method allows the formation of amorphous citrates of metals with a wide flexibility of compositions.[21] Thermal decomposition of these precursors leads to mixed oxides or solid solutions of high homogeneity. In our preparation procedure $ZrO(NO_3)_2$ (Acros 22263) and $Ce(NO_3)_3$ (Fluka 22350) were dissolved in deionized water in such a manner to give solutions of 0.1 M. Citric acid (Merck 244) was added with 10 wt % excess over the stoichiometric quantity for the complete complexation of the metal ions. The solution was partially dehydrated in a rotary evaporator at 40 °C until the appearance of a colorless gel. The viscous material obtained was dried overnight in a vacuum oven set at 70 °C. During this treatment an intense production of nitrogen oxide vapors occurred. A spongy yellowish amorphous citrate was obtained which was subsequently calcined at 450 or 700 °C for 3 h.

There are several external parameters affecting the synthesis and the structure of the final material when the sol−gel method is used. The nature of the solvent, water/alkoxide ratio, acidity, and temperature are particularly important.[22,23] In this work, the starting materials were zirconium tetra-isopropoxide (Fluka 96595) and $Ce(NO_3)_3$ (Fluka 22350). The preparation method was dictated by the low rate of precipitation when no $Ce(NO_3)_3$ was present in 2-propanol. The final procedure was a compromise. Because the formation of the precipitate should not be too long, we set the maturation time at one week. The other condition was to obtain a solid of relatively high surface area after freeze-drying and calcination (here: 70 $m^2\ g^{-1}$ after calcination at 450 °C). The use of nitric acid in the proportion indicated below permitted adjustment of the hydrolysis rate of zirconium tetra-propoxide to these objectives. No other modifier (e.g., acetylacetonate) was used.

The procedure was therefore the following. The cerium salt was dissolved in 2-propanol, and zirconium tetra-propoxide was added to this solution (molar ratio [2-propanol]/[Ce] + [Zr] = 50). The hydrolysis was realized with nitric acid 65% (Merck) which was added dropwise under vigorous stirring so as to have a molar ratio of $[Zr]/[H_2O] = 2.7$, with $[Zr]/[H^+] = 5$.[23] A clear solution was obtained. A gel formed slowly over a 1-wk maturation period. The final gel was freeze-dried at −40 °C. The powders were calcined at 450 °C or 700 °C for 3 h. This was sufficient for the formation of the corresponding tetravalent oxides;[24] namely no hydrogen peroxide was necessary during the room-temperature preparation steps.

Catalyst Characterization. BET specific surface areas (SSA) were measured by adsorption of nitrogen at −196 °C using a Micromeritics ASAP 2000 instrument. Prior to each analysis, 150 mg of powder was outgassed at 150 °C for 2 h at a pressure of 0.1 Pa.

XRD patterns were collected on the freshly calcined samples by means of a Kristalloflex Siemens D5000 diffractometer using the Cu *K*α radiation at $\lambda = 1.5418$ Å. The powders (40−75 μm) were mounted on silicon monocrystal sample holders. Data acquisition was realized in the 2θ range 2−65° with a scan step size of 0.03°. The reflections of certain crystallographic planes were investigated in more detail, using 2θ ranges of 24−40° for (111) and (200) planes and 108−134° for (531) at a scan step size of 0.02°. The in situ evolution of crystallinity was monitored using a standard attachment of the instrument, namely a furnace disposed in the analysis chamber. The samples (40−75 μm), precalcined at 300 °C for 3 h, were mounted on a Pt sample holder and heated from 300 °C to 900 °C at a rate of 1°/s, the spectra being taken every 100 °C after 1 h of stabilization. The 2θ range was 15−70°, with a scan step size of 0.03°.

XPS spectra were recorded on a SSX-100 model 206 Surface Science Instrument spectrometer at room temperature, under a vacuum of 1.33 mPa. Monochromatized Al *K*α radiation ($h\nu$ = 1486.6 eV), obtained by bombarding the Al anode with an electron gun operating at a beam current of 12 mA and an accelerating voltage of 10 kV, was used. The spectrometer energy scale was calibrated using the Au $4f_{7/2}$ peak energy centered at 83.98 eV. The charge correction was made considering that the C1s signal of contaminating carbon (C−C or C−H bonds) was centered at 284.8 eV. The C1s, Zr3d, Ce3d, and O1s levels were chosen for characterization because their signals are the most intense and do not overlap. The composite peaks were decomposed by a fitting routine included in the ESCA 8, 3 D software. For peak deconvolution, peaks were considered to be Gaussian for 85% and Lorentzian for 15%. The baseline was considered linear and tangent to the peak wings. Atomic surface composition was calculated using the sensitivity factors (Scofield) provided by the same software, applied to the surface below the corresponding fitted XPS signals.

Diffuse reflectance infrared Fourier transform (DRIFT) spectra were collected in a Brucker IF S88 spectrometer. The samples were placed in the sample holder without any treatment such as pressure or dilution. The signals were recorded at room temperature, performing 100 scans at a resolution of 4 cm^{-1}.

Environmental scanning electron microscopy (ESEM) images and surface composition evaluation were taken with a XL 30 ESEM-FEG Philips apparatus using an acceleration voltage of 30 kV.

Results

Surface Area Measurements. The evolution of the SSA of the solids as a function of the composition and calcination temperature is shown in Figure 1. The increase of the cerium content leads to a much more regular increase in the SSA for the citrate prepared samples than for the sol−gel samples.

(20) Yashima, M.; Morimoto, K.; Ishizawa, N.; Yoshimura, M. *J. Am. Ceram. Soc.* **1993**, *76*, 1745.
(21) Courty, P.; Ajot, H.; Marcilly, C.; Delmon, B. *Powder Technol.* **1973**, *7*, 21.
(22) Ward, D. A.; Ko, E. I. *Ind. Eng. Chem. Res.* **1995**, *34*, 421.
(23) Parvulescu, V. I.; Bonnemann, H.; Parvulescu, V.; Endruchat, U.; Rufinska, A.; Lehmann, Ch. W.; Tesche, B.; Poncelet, G. *Appl. Catal. A: General* **2001**, *214*, 273.
(24) Ingo, G. M.; Paparazzo, E.; Bagnarelli, O.; Zachetti, N. *Surf. Interface Anal.* **1990**, *16*, 515.

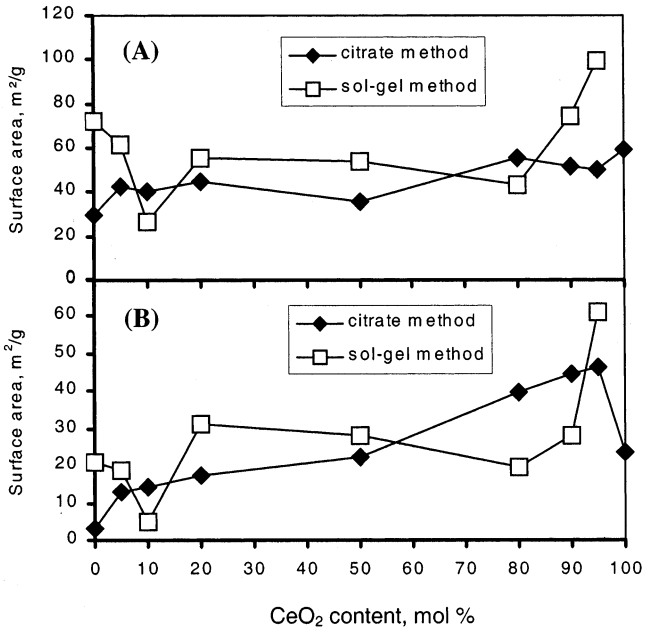

Figure 1. Surface area evolution as a function of composition and synthesis method for the samples calcined at (A) 450 °C and (B) 700 °C.

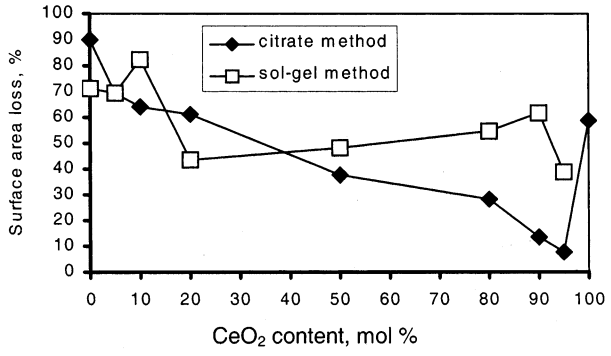

Figure 2. Loss of surface area due to calcination (from 450 to 700 °C) versus composition.

Figure 2 shows the loss of surface area between 450 and 700 °C for both synthesis methods. The thermal stability, reflected by a reduced loss, increases with the Ce content in the samples prepared by the citrate method. Pure oxides do not appear as thermally stable as mixed oxides.

X-ray Photoelectron Spectroscopy. In each case, the carbon signal is deconvoluted into three peaks positioned at 284.6 eV corresponding to carbon involved in C−C and/or C−H bonds, 286.4 eV ascribed to C−O bonds, and 288.6 eV corresponding to O=C−O bonds. The second one could come from 2-propanol used for cleaning the sample holders. The third, centered at 288.6 eV, is due to CO_3^{2-} groups on the surface. Formation of surface carbonates appears to be a consequence of the basicity of both oxides.[25] The oxygen peak can be decomposed into three components: the lower binding energy (BE) one at 529.5 eV corresponds to lattice oxygen, and the higher BE peak at 531.3 eV is due to hydroxyl groups or atmospheric moisture. The third component, at 532.3 eV, corresponds to oxygen of the CO_3^{2-} groups.[26] The Zr3d level splitting is well

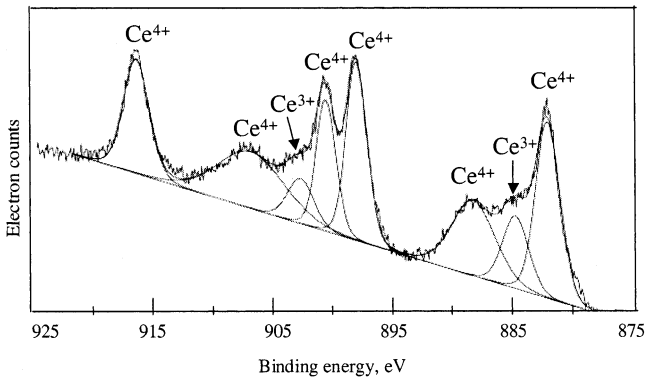

Figure 3. Example XPS spectra in the range of binding energy of Ce3d level; investigated sample $Ce_{0.5}Zr_{0.5}O_2$ prepared by the citrate method and calcined at 700 °C.

defined: the Zr3d5/2 signal is in the 181.7−182.3 eV range, in good agreement with other works.[26,27]

The case of cerium is the subject of controversy with respect to the bands attribution because the signal of the 3d level has a very complicated structure[28,29] (Figure 3). The 3d level is formed by two series' of peaks: 3d5/2 and two very pronounced "shake-up" satellites; and 3d3/2 with the same characteristics. Very often these peaks are asymmetric due to the coexistence of Ce^{3+} and Ce^{4+} ions. Specific Ce^{3+} features are present around 884.9 and 903.7 eV in the Ce3d region. These signals are considered as fingerprints for the existence of some reduced ions.[30] In our case, partial reduction could occur during analysis[31] if the exposure of the sample to the exciting X-ray beam was long, and caused local heating of the sample (Figure 3).

Table 1 presents some characteristics for selected samples as deduced from XPS investigations. The BE of Zr^{4+} remains unchanged, within the precision limits of the measurements. There seems to be some shift, in parallel direction, of the positions of the O1s and Ce3d5/2 lines, although the corresponding difference in BE values is close to the error range of XPS measurements (0.5 eV). The increase in Ce content seems to lower slightly the BE for both oxygen and cerium regardless of the calcination temperature. The second shake-up satellite of Ce3d3/2 (Table 1) shows the same trend. Another feature is the high content of superficial carbon, i.e., more than 30% of the surface atoms are carbon, independently from the preparation method or calcination temperature. Paparazzo et al.[28] also found by XPS a content of 20% carbon atoms in a commercial sample of CeO_2.

DRIFT Measurements. Selected samples were characterized by DRIFT to elucidate the nature of surface carbon detected in high amounts by XPS. Infrared spectra of some samples calcined at 450 °C and 700 °C are presented in Figure 4. Absorption bands in the

(25) Tanabe, K.; Misono, M.; Ono, Y.; Hattori, H. *New Solid Acids and Bases*; Kodansha Ltd.: Tokyo, Japan, 1989; p 365.

(26) Moulder, J. F.; Sticle, W. F.; Sobol, P. E.; Bomben, K. D. *Handbook of XPS*; Chastain, J., Ed.; Perkin-Elmer Corporation: Wellesley, MA 1992.

(27) Theunissen, G. S. A. M.; Winnubst, A. J. A.; Burggraaf, A. J. *J. Mater. Sci.* **1992**, *27*, 5057.

(28) Paparazzo, E.; Ingo, G. M.; Zachetti, N. *J. Vac. Sci. Technol. A* **1991**, *9*, 1416.

(29) Ingo, G. M.; Dal Maschio, R.; Scoppio, L. *Surf. Interface Anal.* **1992**, *18*, 661.

(30) Abi-aad, E.; Bechara, R.; Grimblot, J.; Aboukaïs, A. *Chem. Mater.* **1993**, *5*, 793.

(31) Paparazzo, E. *Surf. Sci.* **1990**, *234*, L253.

Table 1. XPS Investigation Results

method	%Ce mol	calcination temp.	O1s BE (eV)	Zr3d5/2 BE (eV)	Ce3d5/2 BE (eV)	Ce3d3/2 satellite BE (eV)	Ce/Zr theor	Ce/Zr exp	%C atoms
citrate	100	700 °C	529.08		882.27	916.22			38.7
	80	450 °C	529.29	181.93	882.16	916.43	4	3.1	42.6
		700 °C	529.25	181.90	882.11	916.45	4	5.1	39.5
	20	450 °C	529.59	181.87	882.45	916.64	0.25	0.32	38.3
		700 °C	529.65	181.92	882.48	916.63	0.25	0.42	33.8
sol−gel	80	450 °C	529.17	181.73	882.06	916.38	4	7.9	34.2
		700 °C	529.16	181.70	882.03	916.42	4	7.6	36.4
	20	450 °C	529.66	181.98	882.42	916.58	0.25	0.35	35.4
		700 °C	529.60	181.95	882.38	916.60	0.25	0.34	38.6

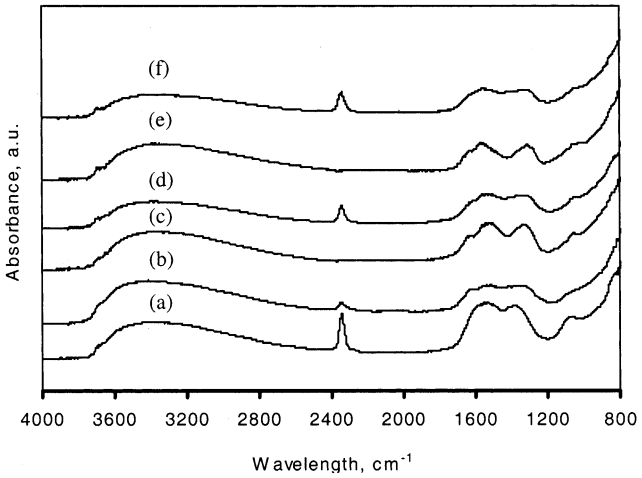

Figure 4. DRIFT spectra for (a) ZrO_2 citrate, 700 °C; (b) $Ce_{0.2}Zr_{0.8}O_2$, sol−gel, 450 °C; (c) $Ce_{0.8}Zr_{0.2}O_2$, citrate, 450 °C; (d) $Ce_{0.8}Zr_{0.2}O_2$, sol−gel, 450 °C; (e) $Ce_{0.8}Zr_{0.2}O_2$, citrate, 700 °C; and (f) CeO_2, citrate, 700 °C.

region 1700−1200 cm^{-1} contain the vibrations of the superficial CO_3^{2-} and OH groups (1600 cm^{-1}). These bands are well-defined.[32] They are also independent from the calcination temperature or the synthesis method. The basicity of these oxides[25] and the thermal treatment performed in air therefore explain the high content of superficial carbon identified by XPS.

ESEM Investigations. ESEM directly allows picturing the material morphology at a resolution substantially better (around 0.5 μm in our case) than conventional ESM. By coupling it with microanalysis, it provides information about the composition of the near-surface zones of the particles to a depth of several micrometers. But the microanalysis (EDX) resolution is comparable to that of conventional electron microprobe analysis (typically 1−2 μm).

For $Ce_{0.2}Zr_{0.8}O_2$-citrate, calcined both at 450 °C and 700 °C, the particles are characterized by an angular shape and the particle size distribution is wide. An overall analysis of the composition revealed a Ce/Zr ratio close to that expected (0.25). The composition may noticeably vary from one grain to another (range 0.25−0.4), but grains of pure oxides were never detected. Composition heterogeneity inside one given grain is not excluded, due to the relatively low resolution of EDX.

A solid of spongy appearance was obtained by the citrate method for $Ce_{0.5}Zr_{0.5}O_2$. Pores of 5−10 μm are shown in Figure 5a. Coupled microanalysis gave particle composition varying in the range Ce/Zr = 0.8−1.4.

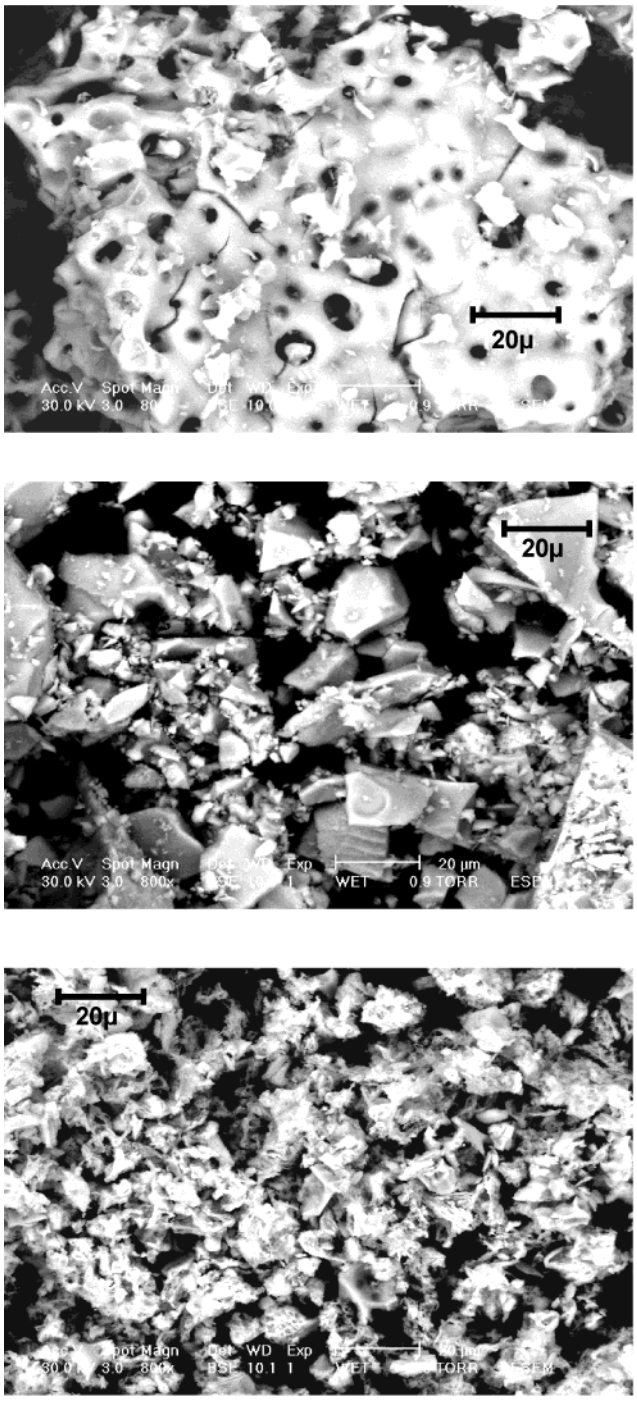

Figure 5. ESEM micrograph for (a) $Ce_{0.5}Zr_{0.5}O_2$ synthesized by citrate method and calcined at 450 °C; (b) $Ce_{0.2}Zr_{0.8}O_2$ synthesized by sol−gel and calcined at 450 °C; and (c) $Ce_{0.8}Zr_{0.2}O_2$ synthesized by sol−gel and calcined at 450 °C.

(32) Terribile, D.; Trovarelli, A.; Llorca, J.; de Leitenburg, C.; Dolcetti, G. *Catal. Today* **1998**, *43*, 79.

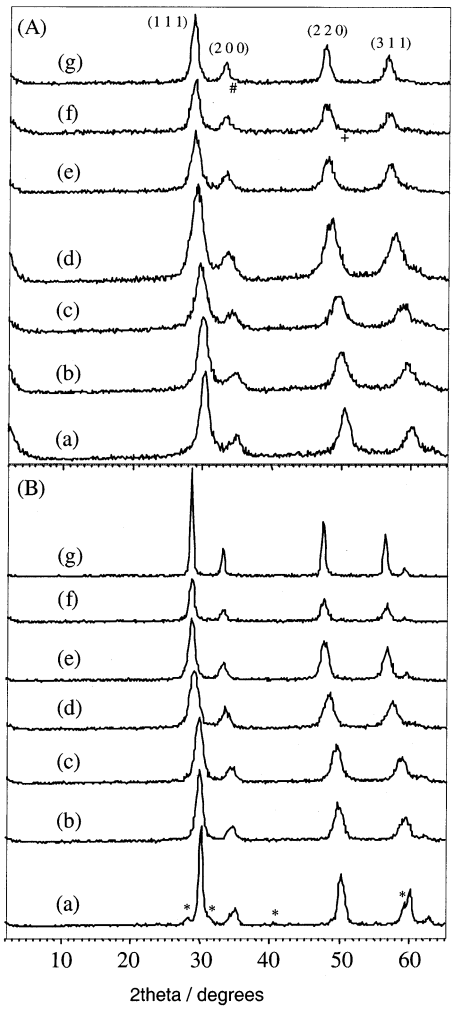

Figure 6. XRD patterns for the solids prepared by the citrate method and calcined at (A) 450 °C and (B) 700 °C: (a) ZrO_2; (b) $Ce_{0.1}Zr_{0.9}O_2$; (c) $Ce_{0.2}Zr_{0.8}O_2$; (d) $Ce_{0.5}Zr_{0.5}O_2$; (e) $Ce_{0.8}Zr_{0.2}O_2$; (f) $Ce_{0.9}Zr_{0.1}O_2$; and (g) CeO_2 (* designates monoclinic ZrO_2).

The same spongy soft-rounded morphology is observed in $Ce_{0.8}Zr_{0.2}O_2$-citrate. For 450 °C the sample seems to be less homogeneous (Ce/Zr = 4−7). After calcination at 700 °C, the Ce/Zr ratio becomes 4−5.6, indicating an improvement of homogeneity.

In the high zirconia composition range ($Ce_{0.2}Zr_{0.8}O_2$), the sol−gel method leads to smaller particles than in the case of the citrate route, but with the same angular morphology (Figure 5b). The Ce/Zr ratio values exhibit little dispersion (0.23−0.28).

Typical angular and faceted large particles (Figure 5c) are observed for high Ce content when using the sol−gel method. This coincides with the observations of Hori et al.[33] $Ce_{0.8}Zr_{0.2}O_2$ is the most inhomogeneous of our samples: instead of the theoretical Ce/Zr ratio of 4, particles with composition ratios varying between 1 and 6.3 were found. The sol−gel route used in this work does not seem advisable for preparing samples with higher contents of Ce. However, no particle of a pure single oxide was observed.

XRD Analysis. *(i) Citrate Method.* The diffractograms are plotted in Figure 6A and B, for 450 °C and 700 °C calcination temperatures, respectively. From pure ZrO_2 to pure CeO_2 (bottom to top in the figures) the expected shift toward lower 2θ angles is confirmed. At the higher calcination temperature (Figure 6B) the narrower diffraction lines indicate a better crystallinity. For pure ZrO_2, the peaks characteristic of the tetragonal phase appear for both calcination temperatures (2θ = 30.2° and 35.2°). After the higher temperature treatment, an additional monoclinic phase appears (designated by * in Figure 6B) with peaks at 28.1° and 31.3°. For $Ce_{0.1}Zr_{0.9}O_2$ calcined at 700 °C, the asymmetry detectable on all signals suggests the presence of the monoclinic phase. By progressively doping ZrO_2 with CeO_2, the tetragonal modification is maintained for a content of ceria of 20% (spectrum c), with no splitting or asymmetry of the peaks being recorded. Going further toward CeO_2 in the scale of composition, the symmetry corresponds increasingly to the cubic one: the (111) reflection shifts from 29.2° for $Ce_{0.5}Zr_{0.5}O_2$ to 28.9° for $Ce_{0.8}Zr_{0.2}O_2$ and 28.6° for CeO_2, in good agreement with the results of Hori.[33] It is striking that the sharpening and increase in the intensity of the reflections observed at 700 °C are more intense for the pure oxides. This confirms that the sintering of the single oxides occurs more easily, as indicated by the surface area evolution with the temperature.

(ii) Sol−Gel Method. Figure 7A and B present the diffractograms for the samples prepared by the sol−gel method. In pure ZrO_2, the monoclinic phase is present starting with calcination at 450 °C (designated by *) and in higher amounts than in the corresponding citrate ZrO_2. It predominates in the samples fired at 700 °C. This phase results from the tetragonal phase transformation.[34] The introduction of Ce atoms maintains the tetragonal structure up to 20% of Ce. The sample $Ce_{0.5}Zr_{0.5}O_2$ (spectrum e) has a cubic symmetry with the (110) and (200) reflections centered at 2θ = 29.4° and 34.05°, respectively. Above this degree of Zr substitution by Ce, two separate phases appear: a cubic CeO_2 (designated by #) with (111) reflection centered at 2θ = 28.6° and a second cubic one (designated +). The position of this latter line corresponds to solids with a Ce/Zr atomic ratio of 1. Yashima et al.[34] showed that for more than 50% mol of CeO_2, heterogeneity in the phase composition appeared. In contrast to the zirconia-rich domain, there is no significant shift of the diffraction lines in the Ce-rich region. One interesting feature is the conspicuously higher diffracted intensities for $Ce_{0.05}Zr_{0.95}O_2$ and $Ce_{0.1}Zr_{0.9}O_2$, both at 450 and 700 °C. It seems that the presence of Ce in the zirconia lattice promotes crystallinity at lower temperature in comparison to that at solids richer in Ce.

(iii) In Situ Evolution of Crystallinity. As can be seen in Figures 8 and 9, there is a constant shift to lower angles as measured for all peaks with the increase of the temperature. This is due to the sample holder dilatation, which consequently changes the position of the sample regardless of the X-ray source and the detector. For this reason, a correction of the peaks position was made on the basis of the Pt (200) line at room temperature, centered at 46.28°.

(33) Hori, C. E.; Permana, H.; Simon, Ng K. Y.; Brenner, A.; More, K.; Rahmoeller, K. M.; Belton, D. *Appl. Catal. B: Environ.* **1998**, *16*, 105.

(34) Yashima, M.; Ohtake, K.; Kakihana, M.; Yoshimura, M. *J. Am. Ceram. Soc.* **1994**, *77*, 2773.

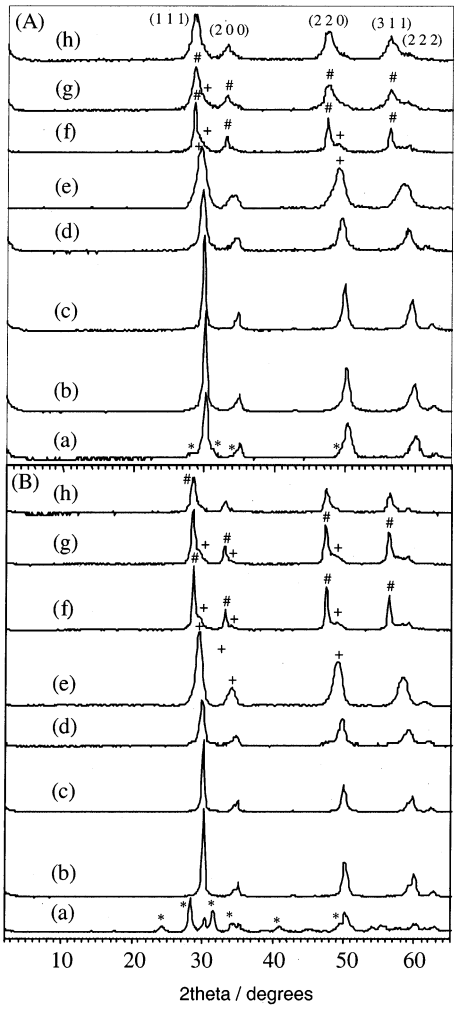

Figure 7. XRD patterns for the solids prepared by the sol−gel method and calcined at (A) 450 °C and (B) 700 °C: (a) ZrO_2; (b) $Ce_{0.05}Zr_{0.95}O_2$ (c) $Ce_{0.1}Zr_{0.9}O_2$; (d) $Ce_{0.2}Zr_{0.8}O_2$; (e) $Ce_{0.5}Zr_{0.5}O_2$; (f) $Ce_{0.8}Zr_{0.2}O_2$; (g) $Ce_{0.9}Zr_{0.1}O_2$; and (h) $Ce_{0.95}Zr_{0.05}O_2$ (*, monoclinic ZrO_2; #, cubic CeO_2; +, cubic $Ce_{0.5}Zr_{0.5}O_2$).

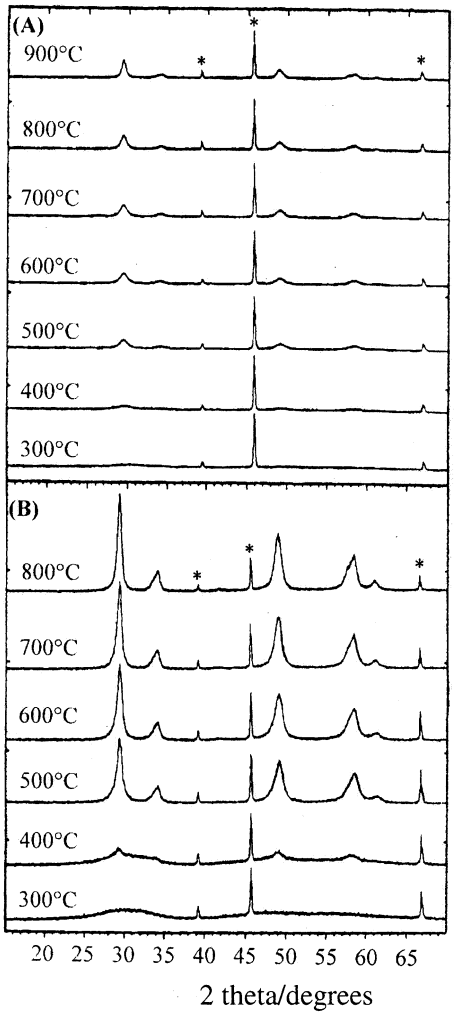

Figure 8. In situ evolution of the crystallinity for $Ce_{0.2}Zr_{0.8}O_2$ samples synthesized by (A) the citrate method and (B) the sol gel method (*, Pt sample holder signal).

For $Ce_{0.2}Zr_{0.8}O_2$ prepared by the citrate method (Figure 8A), the tetragonal structure appears around 400−500 °C ((111) signal centered at 29.75°, after the 2θ correction). The symmetric shape of the reflections indicates a solid solution of the two oxides. In the Ce-rich range of compositions (Figure 9A), the crystallization already begins at 300 °C. The phase is a cubic one, with (111) plane reflection positioned at 28.8°. This corresponds to a solid solution and no segregation of the oxides is detected.

Figures 8B and 9B concern the samples prepared by the sol−gel method. $Ce_{0.2}Zr_{0.8}O_2$ begins to crystallize around 400 °C. A better crystallized tetragonal single phase progressively appears with further increase of the temperature ((111) signal at 29.75° at the same position as for the similar composition prepared by citrate method).

As in the case of the citrate method, sol−gel synthesized $Ce_{0.8}Zr_{0.2}O_2$ exhibits some crystallinity even at 300 °C. The XRD patterns (Figure 9B) show the coexistence of two distinct phases: a cubic CeO_2 ((111) diffraction line at $2\theta = 28.62°$) appears in addition to a tetragonal one. This line appears first as a shoulder of the peak and has a composition close to that of $Ce_{0.5}Zr_{0.5}O_2$ ((111) at $2\theta = 29.3°$). The coexistence of these phases in the samples calcined at 450 °C and 700 °C shows that the present sol−gel procedure is not appropriate for obtaining a homogeneous solid solution, at least when ceria is introduced as nitrate and in high concentration, consistent with the ESEM observations.

(iv) Further Investigations. The above results indicate that the citrate method seems to be able to fulfill our aims. It permits synthesis of materials possessing a fair homogeneity and, correlatively, good thermal stability. Accordingly, further investigations were performed on samples obtained by this method. It actually seemed desirable to pursue the work with the objective to gather more information concerning solid solutions and homogeneity. Another line, namely particle size analysis, seemed less promising. The Scherrer method is unable to bring useful data about the formation of solid solutions. As stated by various authors, several parameters may influence the shape and broadening of the XRD signals, such as particle size and fluctuation of composition (this is mentioned in the discussion section below). Therefore, it is difficult to discard one factor or another. On the other hand, for catalytic purposes, the importance of particle size evaluation is mostly indirect, namely with respect to specific surface area, and the corresponding data have already been presented in section (a) above.

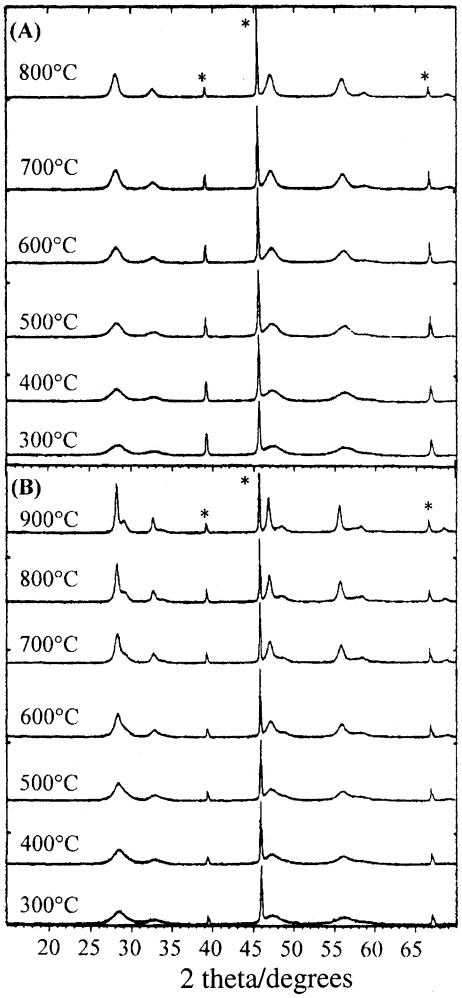

Figure 9. In situ evolution of the crystallinity for $Ce_{0.8}Zr_{0.2}O_2$ samples synthesized by (A) the citrate method and (B) the sol gel method (*, Pt sample holder signal).

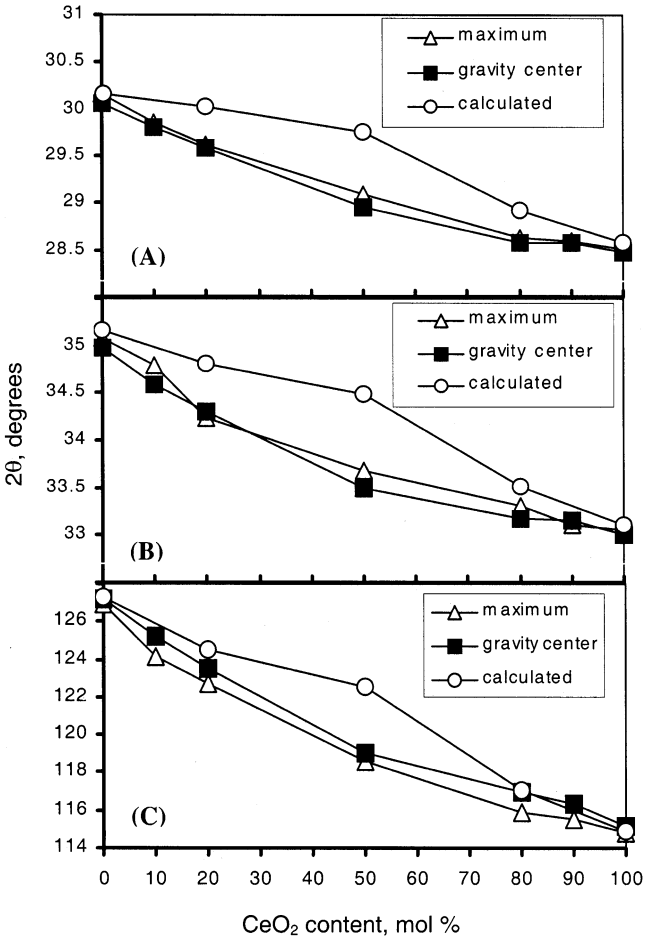

Figure 10. Position of the diffraction line corresponding to (A) (111), (B) (200), and (C) (531) planes for the samples prepared by the citrate method and calcined at 700 °C; 2θ values for the maximum, for the gravity center of the reflection, and calculated.

Our further work consisted of an attempt to evaluate the homogeneity of the solid solutions. The calculation of the unit cell parameters did not show any significant variation for different Ce/Zr ratios. Most articles dedicated to this subject mentioned this kind of investigations (particle size, unit cell) but with no clear conclusions. We, therefore, tried another approach to prove the formation of solid solutions. We performed three different computer simulations to calculate the theoretical patterns. The relative intensity of the main diffraction lines for different Ce/Zr ratios was calculated on the basis of the theoretical position for Ce and Zr in the unit cell. The MSI-CERIUS[2] simulation software, able to calculate the theoretical patterns of perfectly homogeneous CeO_2−ZrO_2 solid solutions, based on the Rietveld method, has been used for this purpose. The basic hypotheses were, in conformity with the X-ray patterns, that CeO_2 and ZrO_2, respectively, crystallize in the cubic and tetragonal system, and the substitution of Ce atoms by Zr modifies significantly the intensity of diffraction of certain planes if the solid solution is formed.

The most intense peak corresponds to the reflection of the (111) crystallographic plane. Two other reflections, (200) and (531), have a significant evolution when passing from pure zirconia to pure ceria: the intensity of the first reflection is diminishing while the second one is increasing.

Comparisons of the theoretical and experimental positions of the reflections are displayed in Figure 10. In each plot there are three curves corresponding respectively to the theoretical position of the reflection ("calculated"), the experimental gravity center position and the position of the maximum of the reflection, as a function of Ce content. For the pure oxides, the structures are well defined at 700 °C, so that almost no difference between the calculated and experimental values is noticed. For the mixed oxides, the calculated diffraction lines are very close to the experimental ones, with the highest discrepancy being observed for $Ce_{0.5}$-$Zr_{0.5}O_2$. Considering the Ce-rich range, there is no significant difference between the position of the gravity center and the maximum of the peaks for the Ce-rich range. This fact shows that the peaks are symmetrical. This indicates that the solid solutions are quite homogeneous in this composition range.

The relative intensity of the (200) line (defined as the ratio between the considered reflection intensity and the most intense one, namely (111)) is very close to the one obtained by computer simulation (Figure 11A). With respect to the position, a slight difference of a maximum of 3% exists compared to the calculated value. The large difference observed in Figure 11B for the (531) reflection is due to the low signal quality in this case, that is

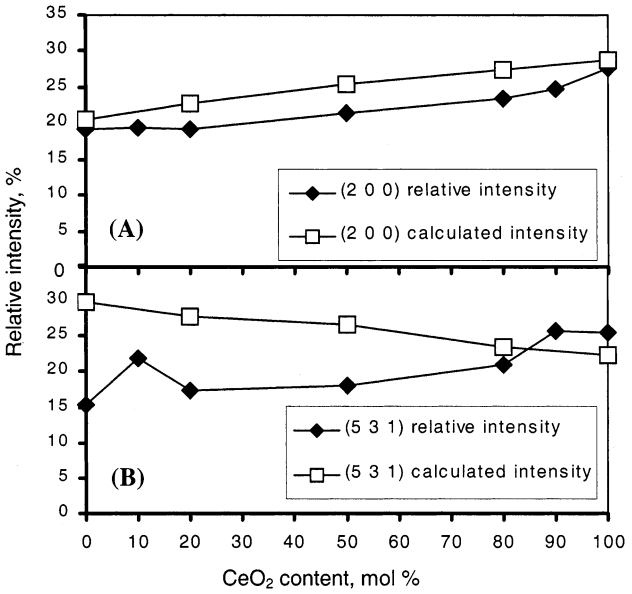

Figure 11. Relative intensity of the plane (A) (200) and (B) (531) reflection (related to (111) peak intensity) for the samples prepared by the citrate method and calcined at 700 °C.

inducing errors in appreciating the broadening or the intensity.

Discussion

There is a general trend to surface area increase with the increase of the ceria content up to 95%. This tendency is practically linear for the more homogeneous samples, namely those prepared by the citrate method. The variations are more complicated in the other case. It seems that the segregated CeO_2 phase, well-identified in the XRD patterns, is responsible for this nonregular behavior. The reason is that pure ceria is sintering more easily. However, the mutual substitution of the two oxides always leads to more stable structures than those of the pure oxides (Figure 2), especially for ceria-rich compositions.

XRD analysis is not very sensitive for detecting fluctuations of composition linked to the existence of small domains with different composition. Because of the high energy of the incident beam, only an average corresponding to the overall bulk composition is obtained. On the other hand, the results of ESEM correspond to a relatively small spatial resolution. Only a1−2-μm depth zone is analyzed. Despite this limitation, ESEM demonstrates that composition exhibits some degree of heterogeneity. XPS probes only a few nanometers in depth but the incident beam is about 1 mm in diameter, substantially larger than the one used in ESEM. Despite their individual limitations, these three tools of investigation are complementary and allow some insight in the structure of our materials.

The monoclinic phase (baddeleyite) is present only in the case of pure zirconia. In the case of sol−gel synthesis this phase appears after calcination at 450 °C, but for the citrate method it appears only at 700 °C. The presence of ceria seems to favor crystallization as ZrO_2 and $Ce_{0.2}Zr_{0.8}O_2$ are X-ray amorphous up to a calcination temperature of 400 °C (Figure 8A) while some crystallinity can be detected at 300 °C for $Ce_{0.8}Zr_{0.2}O_2$ (Figure 9A). For a ceria content in the range of 5−50% the

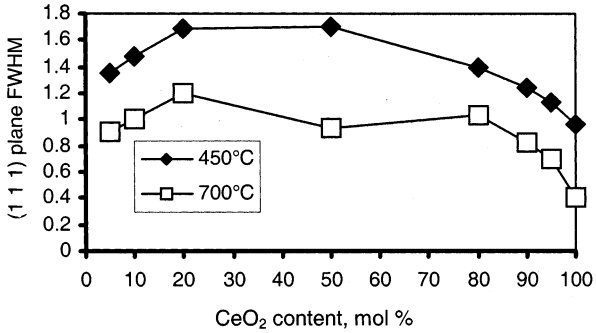

Figure 12. Full-width at half maximum (fwhm) of (111) plane reflection for the samples synthesized by the citrate method and calcined at 450 and 700 °C.

structure is tetragonal, and it is cubic above this range.[19] For the sol−gel synthesized samples, when cerium replaces zirconium in the range 5−50%, a solid solution is obtained (Figure 7). Further increase in ceria content causes the segregation to two phases: one with the cubic structure of CeO_2, and a tetragonal phase characteristic of a solid solution of composition close to $Ce_{0.5}Zr_{0.5}O_2$. The same observation was made by Yashima et al.,[34] who used the sol−gel technique and found a certain degree of heterogeneity when ceria exceeded 50% mol.

On the basis of XRD results, the most homogeneous on the whole range of compositions are the citrate-prepared samples. The citrate method seems to allow the synthesis of real CeO_2−ZrO_2 solid solutions. This conclusion is strengthened by the results of the detailed analysis of specific crystallographic planes. Nevertheless, ESEM shows small fluctuations of composition from particle to particle.

The increase of the ceria content leads to an increased particles size, as shown by ESEM (Figure 5A−C). Even when a solid solution is formed, the morphology is similar to that of the main compound: a spongy soft-rounded shape for high ceria contents and an angular appearance when zirconia is the major component.

The broadness of the diffraction lines of the samples prepared by the citrate method (Figures 6A and 6B) has to be ascribed to the small size of the elementary particles.[4,11] At the same time, small fluctuations in the composition among the particles could lead to a broadening of the reflections.[33] As expected, the full width at half-maximum (fwhm) of the reflection of the (111) plane is decreasing with the increase of the calcination temperature (Figure 12). Passing from Figure 6A to 6B, no shift of the peaks occurs; this is an indication that no phase modification or separation occurs when the crystallite size increases due to sintering. Thus, our results suggest that the broader signal at the lower calcination temperature may be attributed to small-size crystallites. Consequently, the solid solution already exists or its formation begins below 400 °C. On the other hand, the maximum of fwhm obtained for the intermediate compositions in ceria (Figure 12) can be correlated with the microanalysis results. It appears that, in this case, the heterogeneity is responsible for the broadening of the peaks. However, as a consequence of the sintering process, the fwhm decreases. It may be speculated that both effects responsible for signal broadening (small particles existence and variation of composition among the particles) get partially annihilated.

There is little hope to have access to elementary particle size. Direct elementary particle size and identification using TEM seems very difficult because of the interpenetration of numerous crystallites of different orientations in micrometer-size aggregates, very difficult to break.

XPS shows that the superficial distribution of Ce and Zr is unchanged after calcination at higher temperature. Moreover, the Ce/Zr atomic ratio is close to that expected (Table 1). This means the surface and bulk compositions are identical. However, there is one exception, namely $Ce_{0.8}Zr_{0.2}O_2$ prepared by sol−gel. This is another proof of the nonhomogeneity of our oxides in the region of high concentration in cerium when the present sol−gel procedure involving the nitrate precursor is used for synthesis.

The oxygen storage capacity reflects a complex process, involving the adsorption of gaseous oxygen, favored by structural defects. The increase of Zr^{4+} content in the solid solution (Zr^{4+} ionic radius is 0.84 Å, whereas for Ce^{4+} it is 0.97 Å) will decrease the cell volume and will increase the oxygen adsorptive properties of ceria.[13,15,35] On the other hand, the cubic symmetry favors oxygen diffusion through the lattice likely due to an adequate size of the channels for oxygen migration. This explains why high concentrations of CeO_2 in the solid solution are required, since the cubic symmetry is achieved only if the Ce content exceeds 50%. Indeed, when the Ce content increased, a decrease of the binding energy of oxygen was recorded. This behavior is independent from the calcination temperature (Table 1). On the basis of these observations, the following remarks may be made:

(i) The absence of any shift in the binding energy due to calcination proves that the symmetry of the lattice is the same. (ii) X-ray patterns, correlated with the values of the binding energies, suggest the existence of a real solid solution already at 400−450°; (ii) XPS results clearly show the higher mobility and availability of the lattice oxygen in the high concentration range of Ce (Table 1).

Conclusions

The mixed oxide system CeO_2−ZrO_2 was investigated in order to determine the solubility ranges when the calcination temperature is not too high, namely below the temperature regions considered in ceramic science. For low ceria contents, our sol−gel procedure offers the possibility to obtain a homogeneous solid solution. However, an increase of the ceria content (more than 20%) leads to a segregation of phases. Pure ceria and a phase with an approximate composition $Ce_{0.5}Zr_{0.5}O_2$ are obtained. However, this does not exclude that procedures different from the one we used could yield materials with a better homogeneity.

The citrate method lowers the surface areas of the materials with respect to the sol−gel procedure but offers the possibility to obtain solid solutions in a wider range of compositions. Moreover, this method is easy to apply and reproducible. Reciprocal substitution of the two oxides enhances the thermal stability of single oxides, especially in the Ce-rich region.

CM021274J

(35) Ranga Rao, G.; Kašpar, J.; Meriani, S.; Di Monte, R.; Graziani, M. *Catal. Lett.* **1994**, *24*, 107.